Use of the Hardening Soil Model for urban tunnels design

***Nicolas GILLERON*[1,2*]**

[1]*Université Paris-Est, IFSTTAR, COSYS, Marne-La-Vallée, FRANCE*

[2]*Egis, Paris, FRANCE*

ABSTRACT

The Hardening Soil Model introduced in the early 2000's has been widespread in the geotechnical engineering practices as well as in several finite element packages. It is now currently used to design all types of geotechnical structures. We put forward some useful points of vigilance for the geotechnical engineers in the use of this model for studying urban tunnels.

Keywords: Tunnel, Settlement, Finite Element, Constitutive model

1. INTRODUCTION

The constitutive model adopted for the soil in numerical simulations aiming at predicting deformations under service conditions has a strong influence on the results. Taking into account the constructive methods and the geology, the settlement induced by shallow tunnelling is highly dependent on the constitutive model. From linear elastic constitutive models to more complicated ones, numerous formulations have been proposed in the last fifty years. Nevertheless, it is generally admitted that numerical model tends to predict too wide settlement troughs (ITA, 2007) and therefore to minimize differential settlements on building. This paper presents a critical discussion on the constitutive model most commonly used by geotechnical engineers to design structures: the Hardening Soil Model. This model shares some characteristics with others: that's why some points discussed hereafter can be extended to other models. First we introduce the main mechanisms, and then we discuss their consequences on the maximum settlement and the width of the settlement trough. We finally discuss the impact of a variant of the HSM: the HSsmall. All the modelling have been made with PLAXIS 2D 2015.

2. 2D MODELLING OF URBAN TUNNELS WITH THE HSM

2.1. The Hardening Soil Model

The Hardening Soil Model (HSM) has been introduced by (Schanz et al., 1999). It has been integrated in PLAXIS since more than ten years and in other softwares more recently. PLAXIS, ZSOIL and FLAC advise the use of the HSM for

* presenting author

tunnelling modelling. In particular (PLAXIS 2D, 2015) highlights the complementarities between mechanisms which allows to treat a wide domain of soil (graves, sands, silts and overconsolidated clays) as a lot of geotechnical cases (foundations, excavations, tunnels, dams or embankments).

Regarding the tunnelling modelling and the settlement prediction, a lot of case studies in the literature are based on this model ((Janin et al., 2015) or (Möller and Vermeer, 2008) for example). Furthermore, this model is used by French design firms to design urban tunnels.

The HSM is an isotropic elastoplastic constitutive model with a double hardening. It constitutes a synthesis of several models developed in the second half of the twentieth century such as (Duncan and Chang, 1970) or the Cam-Clay (Potts and Zdrazkovic, 2001).

Hereafter is the list of the main mechanism as described in (Plaxis, 2015):

- Plastic straining due to primary compression (compression hardening)
- Plastic straining due to primary deviatoric loading (shear hardening) and hyperbolic stress-strain relationship
- Elastic unloading/reloading
- Failure according to the Mohr-Coulomb failure criterion
- Dependency of the stiffness with the stress following a power law

It considers three elastic stiffness parameters: the unloading/reloading stiffness E_{ur}^{ref}, the secant stiffness in standard drained triaxial test E_{50}^{ref}, the tangent stiffness for primary oedometer loading E_{oed}^{ref}. The other parameters are the failure ratio R_f, Poisson's ratio for unloading/reloading ν_{ur}, a reference value for stresses p_{ref}, the power for stress-level dependency m and the three parameters of Mohr-Coulomb failure criterion: the cohesion c, the angle of internal friction φ, the angle of dilatancy ψ.

Several parameters have hand in more than one mechanism, which makes it difficult to interpret their role in each mechanism and predict the result of a sensitivity analysis.

2.2. Definition of a reference case

We consider, in plane strain, a circular tunnel with a diameter of 10 m, the axis depth being 20 m, in a homogeneous soil in drained conditions. The mechanical parameters, typical for a sand of the Paris, are defined in Table 1 for the HSM and Table 2 for a linear elasticity with Mohr-Coulomb failure criterion. The stress dependent stiffness mechanism has been deactivated by chosen a value of 0 for the *m* parameter. The soil unit weight is equal to 20 kN/m^3. The lateral extension of the mesh is equal to 45 m and the model depth is equal to 35 m. The tunnelling process is simulated with the stress relaxation method, which is the most used for settlements predictions (Wedekin et al., 2012). We increase the stress relaxation factor λ by successive steps until the calculation no longer converges. We didn't model the lining influence, because the largest part of the settlements is created before the lining is built.

Table 1. HSM parameters

K_0 (-)	c (kPa)	φ (deg)	ψ (deg)	E_{ur}^{ref} (MPa)
0,7	10	25	5	100

$E_{50}^{ref}=E_{oed}^{ref}$ (MPa)	R_f (-)	ν_{ur} (-)	m (-)	p_{ref} (kPa)
33	0,9	0.2	0	100

Table 2. Linear elastic parameters

K_0 (-)	c (kPa)	φ (deg)	ψ (deg)	E (MPa)	ν (-)
0,7	10	25	5	100	0.2

Figure 1 describes the initial state of soil regarding the two hardening mechanisms. The plain straight line, with

"+" symbols, shows the initial stress state at different depths. The two yield loci are drawn for a point located at the depth of the tunnel axis (20 m). Since the angle of internal friction is equal to 30°, K_0^{NC} is equal to 0.5 (following Jaky's formula as recommended). K_0^{NC} is lower than K_0 meaning the soil is lightly overconsolidated. The initial stress state is not located on the initial shear yield locus; on the other hand, it is located on the initial compression yield locus.

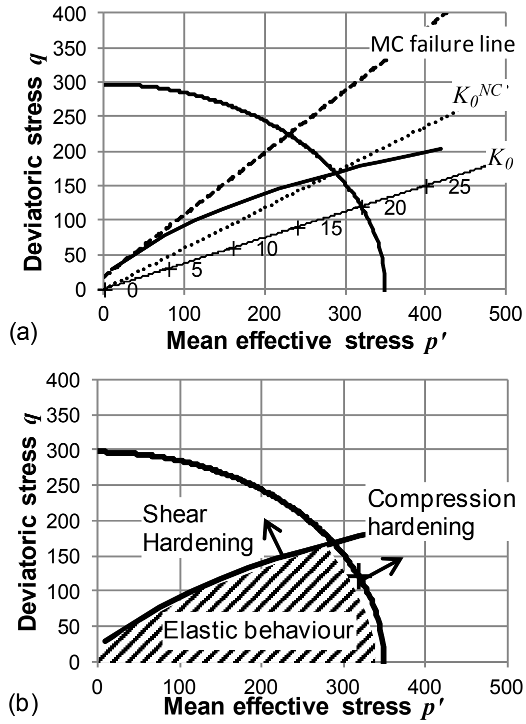

Figure 1. Yield loci at initial stress state in (p',q) plane

In Table 3, the maximum settlement and the trough width parameter K are given for each relaxation step. K is defined as the ratio between the distance where settlement is equal to 60 % and the depth. The maximum settlement is highly non-linear and the settlement trough is wider than the recommended value of 0.35 for sand by (O'Reilly and New, 1982).

Figure 2 shows the area where plastic strains occur and the type of hardening for four values of the relaxation factor: 10 %, 30 %, 50 %, 65 %.

At 10 % of stress relaxation, almost the totality of soil is concerned by the compression hardening. This results from the fact that the initial stress state is on the cap yield locus, so that a slight increase of mean or deviatoric stress is enough. At the crown and at the invert the soil remains elastic because the deviatoric stress and the mean stress are decreasing.

At 30 % of stress relaxation, the shear hardening has begun at sidewall. It is combined with the compression hardening. This hardening is associated with a strong acceleration in maximum settlement (+ 3.2 between 0 to 10 % and + 5.8 between 20 to 30 %).

At 50 % of stress relaxation, there is still an elastic zone under the invert and above the crown. From the sidewall the shear hardening spreads towards the surface in an "ear" shape.

After 65 % of stress relaxation, the Mohr-Coulomb failure criterion is reached on the side wall. The shear hardening is now also developing above the tunnel.

Table 3. Settlement trough profile

λ (%)	10	20	30	40
S_{max} (mm)	3.2	7.2	13.0	21.6
ΔS_{max} (mm)	+3.2	+4.8	+5.8	+8.5
K	0.70	0.69	0.69	0.68

λ (%)	50	60	65
S_{max} (mm)	35.6	62.8	89.0
ΔS_{max} (mm)	+14.0	+17.3	+26.2
K	0.63	0.60	0.56

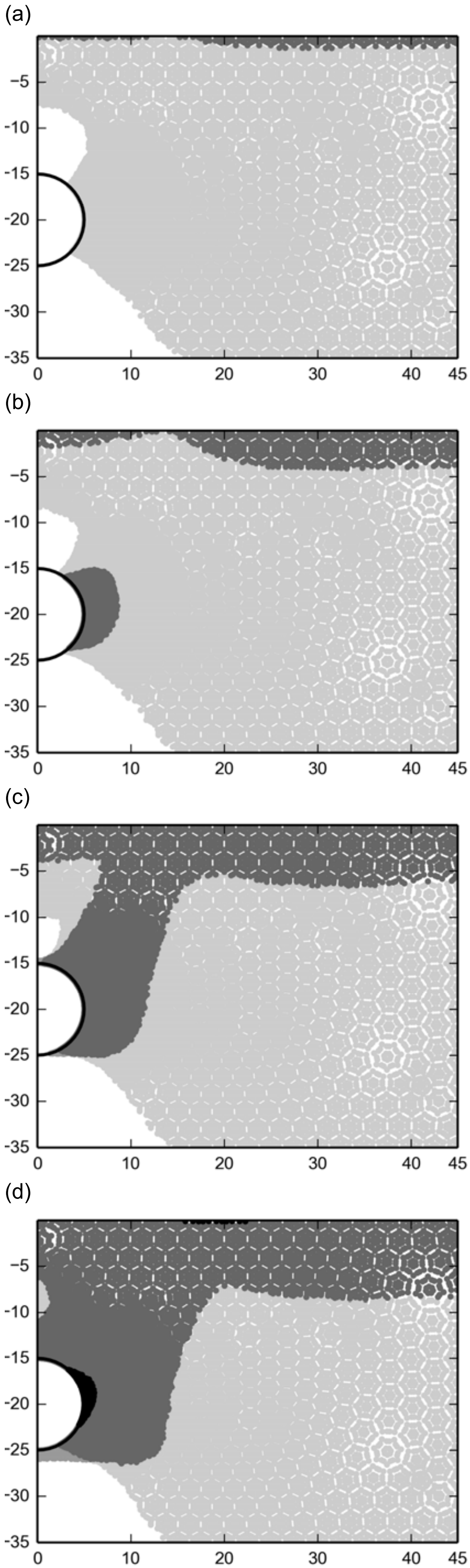

White:	Elastic behavior
Light gray:	Compression hardening
Gray:	Shear hardening
Dark gray:	Comp. + shear hardening
Black:	Failure

Figure 2. Plastic area for different values of the stress relaxation factor (a) 10% (b) 30 % (c) 50 % (c) 65 %

3. DISCUSSION

3.1. Compression hardening

The initial stress state is located on the yield locus by construction of the model. A slight increase of the hardening parameter p^{eq} by an increase of shear or mean stress activates this mechanism (eq. (1)).

$$p^{eq} = \sqrt{\frac{q^2}{M^2} + (p')^2} \quad (1)$$

In the case discussed here, plastic straining starts from the first step of relaxation. The settlements calculated with the HSM are more than twice larger than those calculated with the elastic perfectly plastic model (Table 4). The settlement trough is also wider with the HSM. Indeed, strains are higher where the mechanism is activated, on the sidewall. Near the crown and the invert, the soil has an elastic behavior, associated with the unloading/reloading stiffness which is three times higher than the tangent stiffness at the early stage of the plastic regime.

The model permits to consider a previous overburden pressure. With a very small overburden pressure of 50 kPa, deformations are divided by two, very close to those obtained in linear elasticity (Table 4).

Deformations at this step are small compared to next steps and final ones. The effect of volumetric hardening is no more visible when the stress relaxation increases and the shear hardening becomes more significant.

Table 4. Influence of volumetric hardening

	S_{max} (mm)	K
Hardening Soil Model	3.2	0.70
Linear elasticity	1.5	0.625
HSM + overburden pressure of 50 kPa	1.5	0.625

3.2. Shear hardening

The shear hardening mechanism has been built to reproduce the hyperbolic relation introduced by (Duncan and Chang, 1970) between the axial strain ε_1 and the deviatoric stress q in the context of a triaxial test as:

$$\varepsilon_1 = \frac{q_a}{E_i}\frac{q}{q_a - q} \qquad (2)$$

The initial tangent stiffness E_i is given by:

$$E_i = \frac{2E_{50}}{2 - R_f} \qquad (3)$$

and the asymptotic deviatoric stress by:

$$q_q = \frac{q_f}{R_f} \qquad (4)$$

where q_f, is the failure stress:

$$q_f = (c\cos\varphi + \sigma'_3 \sin\varphi)\frac{2}{1 - \sin\varphi} \qquad (5)$$

E_{50} is the secant stiffness at 50 % of the deviatoric stress q_f (when q=q_f/2, $\varepsilon_1 = q / E_{50}$).

It is possible to get an estimation of the tangent stiffness at the activation of the shear hardening, when the yield locus is reached at 20 m depth. Figure 3 shows the hyperbolic shape and the result of a simulation of a triaxial test using HSM with PLAXIS. We highlight the initial value of the deviatoric stress q_i, 120 kPa, and the deviatoric stress $q*$, 169 kPa, when the yield locus is reached. The failure stress q_f is equal to 441 kPa and initial tangent stiffness E_i is equal to 60 MPa. The numerical and theoretical curves are sufficiently close to evaluate the tangent stiffness by derivation of the hyperbolic formula (eq. (6)):

$$E_t = \left(\frac{d\varepsilon_1}{dq}\right)^{-1} = E_i(\frac{q}{q_a} - 1)^2 \qquad (6)$$

The initial tangent stiffness is equal to 25 MPa, four times lower than the elastic unloading/reloading stiffness, and decreases with the increase of deviatoric stress until 5 MPa when q is equal to 80 % of q_f. In soils where the initial pressure at rest is low, the initial deviatoric stress high, a great care has to be managed when defining parameter E_{50}. It is not equal to the tangent stiffness and the tangent stiffness will be also very different from the unloading/reloading stiffness.

It is remarkable that this formulation involves significant variations of stiffness in the soil but with little consequences on the width of the settlement trough, even if it modifies significantly the maximum settlement.

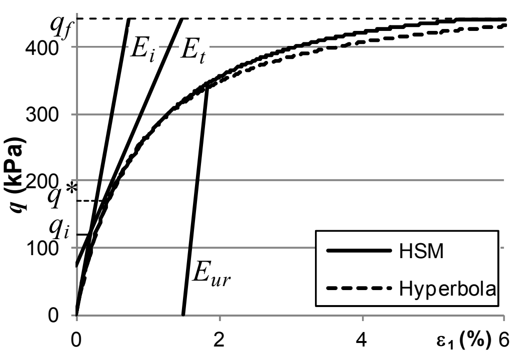

Figure 3. Triaxial test - HSM and hyperbola

3.3. Failure mechanism

The shear hardening limits the increase of the deviatoric stress close to the tunnel. Consequently, the Mohr-Coulomb failure criterion is reached for larger values of the stress relaxation factor. The criterion is reached at 60 % with the HSM and at 35 % with the linear elasticity with Mohr-Coulomb failure criterion (Figure 4). Near the crown, since the behavior is mainly elastic, the HSM has no significant impact (Figure 5).

The plastic strains have no significant consequences on the settlement trough width.

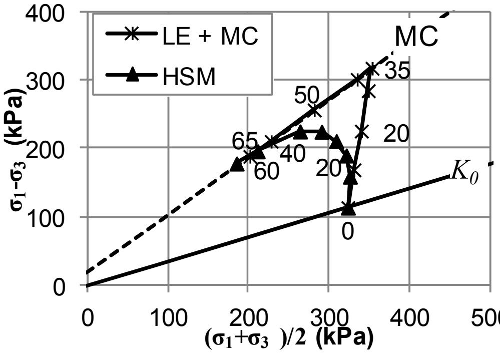

Figure 4. Stress path at the sidewall

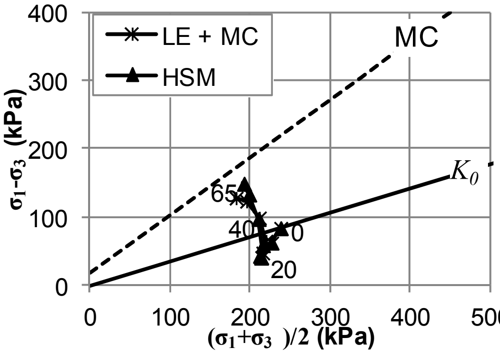

Figure 5. Stress path near the crown

3.4. Unloading/reloading modulus

The unloading/reloading stiffness is at least equal to the tangent initial modulus E_i to permit the calculation of the shear hardening parameter.

Two zones are concerned by unloading/reloading. A small one is located just above the tunnel, the second one under the raft.

The presence of a stiff zone above the crown does not imply a lower level of settlement. The settlements are mainly due to the shear hardening starting from the sidewall. Under the raft the unloading/reloading mechanism permits to avoid the uplift of the tunnel which occurs with linear elastic law, which is very relevant. This remark is also one strong argument to use HSM for designing shafts.

3.5. Power law stiffness dependency

Until this point, the power law stress dependency has been deactivated by setting the parameter m of the model to zero. Here we discuss the influence of this mechanism and why it leads to difficulties in the shallow tunnel context.

Following classical geotechnical considerations, the model aims at expressing the dependency between the soil stiffness and the confining stress. The three moduli of the HSM are concerned with the type of dependency, hereafter written for the unloading/reloading stiffness (eq.(7)):

$$E_{ur} = E_{ur}^{ref} \left[\frac{c.\cos\varphi + \sigma_3 \sin\varphi}{c.\cos\varphi + p_{ref} \sin\varphi} \right]^m \qquad (7)$$

The unloading/reloading stiffness and the shear stiffness depend of the minor principal stress σ_3; the oedometric stiffness depends of the major principal stress (at least at the initial state).

The parameter p_{ref} gives the stress level for which the modulus is equal to its reference value. PLAXIS recommends p_{ref} equal to 100 kPa. This value brings to at initial stiffness equal to the reference value at a depth between 5 and 10 m depending on K_0. The power law parameter m is advised between 0.5 and 1. The parameters c and φ have also an influence. If the cohesion is very high, or if the internal friction ratio is low, the modulus is equal to the reference value.

This means that the stiffness profile with stress is highly dependent from the failure parameters. We cannot discuss their role independently. We could easily manage the dependence with stress with a power law with more simple coefficients. Furthermore the dependency with the minor principal stress is redundant with the shear hardening in the case of shallow tunnel. Indeed in the vicinity of the excavation the increase of deviatoric stress is due to the decrease of minor principal stress. So both mechanism are concerned and both leads to a reduction of stiffness.

On the settlement trough width, it is noticed that an increase of stiffness with depth, or confining stress, leads to narrower settlement trough. Yet this effect is not sufficient to obtain trough as narrow as the empirical ones.

3.6. HSsmall version

The Hardening Soil Model with small-strain stiffness (HSsmall) has been introduced by (Benz, 2007). It permits to take into account a higher stiffness for very low strains.

To test this model, we followed the values of (Hejazy et al., 2008) to define the two new parameters, the initial shear modulus G_0 and the shear strain level $\gamma_{0.7}$. G_0 is equal to 1.5 times the G_{ur} value 65 MPa and $\gamma_{0.7}$ is equal to 10^{-4}.

At 10% of relaxation, the maximum settlement is reduced (S_{max} is equal to 2.6 mm against 3.2 mm) and the settlement trough is slightly narrower ($K = 0.68$ instead of 0.70). At this stage the strains are globally low in soil and the secant stiffness is higher, from 10 m from the sidewall thanks to HSsmall (Figure 6).

From 30 % of relaxation the impact is negligible on both the maximum settlement and the trough width.

The model does not converge at 65 %, this formulation is less stable numerically.

With much higher values of G_0, such as those adopted by (Möller & Vermeer, 2008) the same effect occurs qualitatively for higher values of the relaxation factor.

Nevertheless this formulation has two main difficulties for an engineering use in shallow tunnel. The determination of the two parameters is very uncertain and even if the low strain have undoubtedly a role in the maximum settlement, the settlement have to be managed when strains are significant namely when HSsmall has no impact.

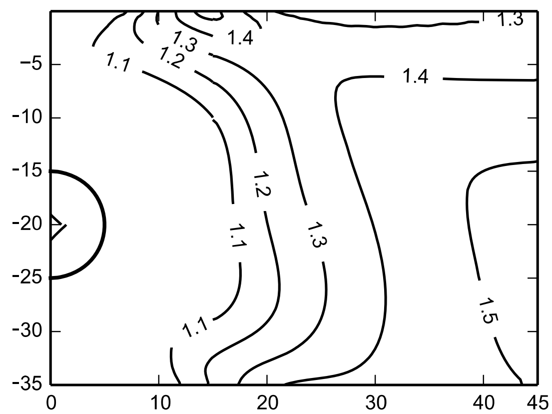

Figure 6. Isovalues of G_S / G_{ur} after 10 % of stress relaxation

4. CONCLUSIONS

The formulation of Hardening Soil Model has several consequences for the study of settlements induced by urban tunnelling. The compression hardening is activated as soon as relaxation forces are applied even if the solicitation is mainly shear. The shear hardening conducts to a tangent modulus much lower than the input parameters E_{50} and E_{ur} and to highly non-linear displacements regarding the stress relaxation factor. With this constitutive model, the failure according to Mohr-Coulomb criterion is also delayed. The formulation of the dependency of stiffness with stress with a power law has a complex influence which is difficult to anticipate on stiffness. The HSsmall does not improve significantly the shape of the settlement trough and it seems difficult to define the additional parameters.

It could be interesting to propose a constitutive model which avoids having too much interdependence between mechanisms. The more relevant aspects of HSM could be used for the study of urban tunnelling: decrease in stiffness with increase in shear stress, taking into account unloading/reloading stiffness and the dependency of stiffness on confining level.

ACKNOWLEDGEMENTS

Thanks to Emmanuel Bourgeois from IFSTTAR and Adrien SAITTA from EGIS for their support and advices. Thanks to the members of the NEWTUN project funded by the *Fond Unique Interministériel*.

REFERENCES

Benz, T.(2007) “Small-strain stiffness of soils its numerical consequences”, Phd Thesis, Universität Stuttgart.

Duncan J. M., Chang C. Y. (1970). “Nonlinear analysis of stress and strain in soil” Journal of the Soil Mechanics and Foundation Division, vol. 96, n°5, 1629-1653.

ITA, (2007) “Settlements induced by tunneling in Soft Ground”. Tunnelling and Underground Space Technology, vol. 22, 119-149.

Janin J., Dias D., Emeriault F., Kastner R., Le Bissonnais H., Guilloux A. (2015). “Numerical back-analysis of the southern Toulon tunnel measurements : A comparison of 3D and 2D approaches”. Engineering Geology, vol. 195, 42-52.

Hejazi, Y., Dias, D., Kastner, R. (2008) “Impact of constitutive models on the numerical analysis of underground constructions”. Acta Geotechnica, vol.3, 251-258.

Möller S.C., Vermeer P.A. (2008). “On numerical simulation of tunnel installation” Tunnelling and Underground Space Technology, vol.23, 461-475.

O’Reilly M.P., New B.M. (1982). “Settlements above tunnels in the United Kingdom – their magnitude and Prediction”. Tunnelling, vol. 82, 173-181.

PLAXIS 2D (2015). “Material Models Manual”.

Potts D. M., Zdravkovic L. (2001) “Finite element analysis in geotechnical engineering : application”. Thomas Telford, London.

Schanz T., Vermeer P.A., Bonnier, B.G. (1999) “The hardening soil model: formulation and verification”. Beyond 2000 in Computational Geotechnics, Balkema, 281-290, Rotterdam.

Wedekin, V., Kastner, R., Guilloux, A., Bezuijen, A., Standing, J., & Negro Jr, A. (2012). “Urban tunnels in soft ground : Review of current design practice”. Geotechnical Aspects of Underground Construction in Soft Ground. London: Taylor & Francis Group.1047-1064 eds: Viggiani